Toward Accurate Diagnosis of White Matter Pathology Using Diffusion Tensor Imaging

M. D. Budde[1], J. H. Kim[1], H-F. Liang[1], R. E. Schmidt[1], J. H. Russell[1], A. H. Cross[1], S-K. Song[1]

[1]Washington University, St Louis, MO, United States

Introduction

Diffusion tensor imaging (DTI) can provide detailed information regarding the microstructural organization of central nervous system white matter. However, the underlying pathological correlates of diffusion changes have not been adequately determined. In this report, we investigate two animal models of injury to spinal cord white matter to perform a quantitative comparison between axial ($\lambda_{\parallel}$) and radial ($\lambda_{\perp}$) diffusivities derived from DTI and histological markers of axon and myelin injury by incorporating a procedure to register the histological images to MRI[1] and applying receiver operating characteristic (ROC) analyses.

Methods

Mice were induced with either experimental autoimmune encephalomyelitis (EAE) or spinal cord contusion injury (SCI). EAE mice underwent *in vivo* DTI with the following parameters: TR=1.5s, TE=49 ms, Δ=25 ms, δ=10 ms, signal averages=4, slice thickness=1.0 mm, FOV=1 cm2, data matrix 128 x 128 (zero filled to 256 x 256), b-values of 0 and 0.785 ms/μm^2. DTI parameter maps were calculated for $\lambda_{\parallel}$, $\lambda_{\perp}$, RA, and trace. Spinal cords from mice with SCI underwent *ex vivo* DTI with identical parameters as those *in vivo* except for the following: TE=30 ms, Δ=12 ms, δ=4 ms, signal averages=8, slice thickness=0.75 mm, b-values of 0 and 1.813 ms/μm^2.

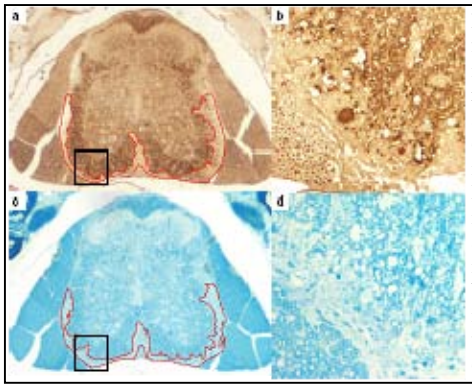

Figure 1. Immunostaining for phosphorylated neurofilaments (SMI-31) revealed axonal damage along the subpial contour of the ventrolateral white matter (a & b). Demyelination was evident in the similar region in an adjacent slice stained for myelin using Luxol fast blue (c & d). Regions of interest were manually traced to outline the region of injury (a & c).

Fixed spinal cord sections were stained for myelin with Luxol fast blue (LFB)-Periodic acid-Schifff (PAS) and for axons using a primary antibody for phosphorylated neurofilaments (SMI-31, Sternberger Monoclonals Inc.). Histological images were down-sampled to the resolution of the DTI and warped using a thin-plate spline warping algorithm to correct for fixation-induced tissue distortions. All image processing procedures were written in Java and implemented as plugins in ImageJ[2].

Regions of interest (ROIs) were drawn on the original histological images, one outlining the entire ventrolateral white matter, and one outlining either the region of axonal injury or demyelination (Fig. 1). ROIs were transformed using the previously computed registration parameters and were applied to the DTI parameter maps for subsequent analysis (Fig. 2). ROC curves and the area under each ROC curve (A_z) were computed for RA, $\lambda_{\parallel}$, $\lambda_{\perp}$, and trace.

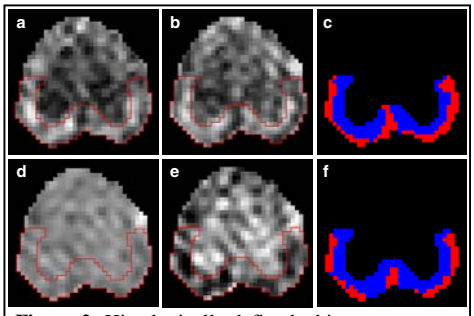

Figure 2. Histologically defined white matter regions were registered and warped to DTI parameter maps for RA (a), $\lambda_{\parallel}$ (b), trace (d), and $\lambda_{\perp}$ (e) and color coded for a better visualization: axonal damage (c; red – damaged axons; blue – spared axons) and demyelination (f; red – demyelination; blue – spared myelin).

Results

The ventrolateral white matter in the spinal cord of mice with EAE contains both axonal damage and demyelination along the pial surface of the white matter and the two injury types substantially overlap (Fig. 2). A_z for axonal injury, $\lambda_{\parallel}$ (0.79), $\lambda_{\perp}$ (0.69), RA (0.77), and trace (0.55) is therefore similar to those for the demyelination, $\lambda_{\parallel}$ (0.71), $\lambda_{\perp}$ (0.69), RA (0.73) and trace (0.50) (Fig. 3). In the region of injury defined by SMI-31 and LFB, $\lambda_{\parallel}$ was decreased and $\lambda_{\perp}$ was increased compared to the normal appearing white matter.

Significant axonal damage is evident in the ventrolateral white matter at the sit e of injury one day following SCI. A region of axonal preservation exists along the subpial contour of the cord with significant axonal damage present in the interior white matter. A_z for axonal damage was greater for $\lambda_{\parallel}$ (0.94), trace (0.92), and RA (0.87) compared to $\lambda_{\perp}$ (0.49). $\lambda_{\parallel}$ decreased in the region of axonal damage compared to the region of axonal preservation, whereas there was no change in $\lambda_{\perp}$. At one day post-injury there was no evidence of myelin loss based of LFB staining, so ROC curves were not computed.

By seven days post-injury, both axonal damage and myelin loss were present at the site of injury, but demonstrated regional differences. A_z for axonal damage was greater for RA (0.80) and $\lambda_{\parallel}$ (0.78) than for $\lambda_{\perp}$ (0.58) and trace (0.60). In the region of axonal damage, $\lambda_{\parallel}$ decreased compared to the region of axonal preservation, while there was no change in $\lambda_{\perp}$. A_z for myelin loss was greater for $\lambda_{\perp}$ (0.90), RA (0.88), and trace (0.82) than for $\lambda_{\parallel}$ (0.62). In the region of significant myelin loss, $\lambda_{\perp}$ increased compared to the region of spared white matter, while $\lambda_{\parallel}$ was unchanged.

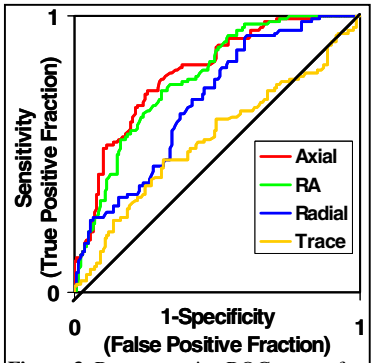

Figure 3. Representative ROC curves for each of the DTI parameters in detecting the region of axonal damage identified by histology for the EAE mouse spinal cord. Both RA and $\lambda_{\parallel}$ detect axonal injury in this example.

Discussion

In EAE, regions of axon and myelin injury significantly overlap, but $\lambda_{\parallel}$, $\lambda_{\perp}$, and RA are similar in their detection of the two types of white matter derangement. $\lambda_{\parallel}$ decreases and $\lambda_{\perp}$ increases in the region of injury, demonstrating that $\lambda_{\parallel}$ and $\lambda_{\perp}$ are sensitive to the differential pathologies. A decrease in RA is sensitive to the region of injury, but is not specific to the pathology. Trace (equal to the sum of $\lambda_{\parallel}$ and $2\lambda_{\perp}$) is least effective.

In contrast, when there are regional differences in axonal and myelin injury, $\lambda_{\parallel}$ and $\lambda_{\perp}$ predict the injury type with high accuracy. $\lambda_{\parallel}$ is good predictors of axonal damage but not myelin loss. $\lambda_{\perp}$ is a good predictor of myelin loss but not of axonal damage. Therefore, the dissociation between the two directional diffusivities and the two types of white matter injury demonstrates that a decrease in $\lambda_{\parallel}$ and an increase in $\lambda_{\perp}$ are sensitive and specific to detect axonal damage and demyelination, respectively. Although a decrease in RA is sensitive to injury, it was not specific to the underlying pathology of either axonal damage or demyelination.

Conclusions

Establishing a relationship between pathology and magnetic resonance is essential for correctly interpreting and validating MR findings. The proposed method of quantitatively comparing histology and MRI incorporates a registration algorithm to obtain a one-to-one pixel correspondence between the two modalities and further employs an ROC analysis to quantify the correspondence of DTI parameters with histologically defined regions of axonal damage and demyelination. The results further support the hypothesis that decreased $\lambda_{\parallel}$ and increased $\lambda_{\perp}$ are surrogate markers of axonal and myelin damage, respectively[3].

References

1. Breen, M. S., et al. *Comput Med Imaging Graph* 29, 405-17 (2005).
2. Rasband, W.S., ImageJ, U.S. NIH, http://rsb.info.nih.gov/ij/, (1997-2005).
3. Song, S. K. et al. *Neuroimage* 20, 1714-22 (2003).